Effect of single-site mutations on hydrophobic-polar lattice proteins

Guangjie Shi, Thomas Vogel, Thomas Wüst, Ying Wai Li, and David P. Landau

Phys. Rev. E **90**, 033307 — Published 15 September 2014

DOI: 10.1103/PhysRevE.90.033307

Effect of Single-Site Mutation on HP Lattice Proteins

Guangjie Shi,[1] Thomas Vogel,[2] Thomas Wüst,[3] Ying Wai Li,[4] and David P. Landau[1]

[1] *Center for Simulational Physics, The University of Georgia, USA*
[2] *Theoretical Division (T-1), Los Alamos National Laboratory, Los Alamos, NM 87545, USA*
[3] *Scientific IT Services, ETH Zürich, 8092 Zürich, Switzerland*
[4] *National Center for Computational Sciences, Oak Ridge National Laboratory, Oak Ridge, TN 37831, USA*

(Dated: August 18, 2014)

We developed a heuristic method for determining the ground-state degeneracy of hydrophobic-polar (HP) lattice proteins, based on Wang–Landau and multicanonical sampling. It is applied during comprehensive studies of single-site mutations in specific HP proteins with different sequences. The effects in which we are interested include structural changes in ground-states, changes of ground-state energy, degeneracy, and thermodynamic properties of the system. With respect to mutations, both extremely sensitive and insensitive positions in the HP sequence have been found. That is, ground state energies and degeneracies, as well as other thermodynamic and structural quantities may be either largely unaffected or may change significantly due to mutation.

Keywords: HP Model, Wang-Landau Sampling, Mutation, Ground State

I. INTRODUCTION

The protein folding problem has been studied for more than 50 years, but much remains to be learned. One of the fundamental remaining questions is: "How is the 3D native structure of a protein determined by the physicochemical properties that are encoded in its 1D amino-acid sequence?" [1] Scientists used to believe that any two naturally occurring proteins with a 40% or higher sequence identity would possess the same fold [2]. However experiments discovered that proteins such as *Pfl6* and *Xfaso 1* with high sequence similarity end up with different folds [3]. Furthermore, Alexander *et al.* have successfully designed two proteins that share 88% of their sequence, but fold into totally different tertiary structures [4]. More generally, it was recently experimentally confirmed that small local differences can lead to large changes in the global organization of amino acid sequences [5]. To understand these phenomena better, a first step is to investigate how the change of a single amino acid affects higher order structure and functions of a protein. Experimental studies of single amino acid substitutions on *lac* repressor [6], for example, showed that proteins often keep phenotypically silent for about 50% of such substitutions. However, very sensitive positions in the amino-acid sequence also exist [7].

The understanding of the protein folding problem has been enhanced through studies of generic, coarse-grained models [8, 9]. The simplest one is the hydrophobic-polar (HP) lattice model [10, 11] which has been used in several problems of biological interest, such as surface adsorption [12–16] and protein folding in membranes [17] or confined environments [18, 19]. Despite the simplicity of the HP model, finding the lowest energy structure of a given sequence is an NP-complete problem [20]. For long sequences (chain length $\gtrsim 30$), enumeration methods (see, e.g., [21–23]) are not accessible. However, different folding algorithms and Monte Carlo methods have been developed for approaching this problem. Examples include, but are not limited to, constraint-based approaches [24], chain-growth methods [25, 26], in particular the pruned-enriched Rosenbluth method (PERM) and its variants [27–31], sequential importance sampling [32], fragment regrowth Monte Carlo [33], multidomain sampler [34], genetic algorithms [35, 36], evolutionary Monte Carlo [37], and ant colony models [38]. Among those, the sampling method developed by Wang and Landau [39] has shown to be powerful and highly precise in simulating proteins and polymers [40, 41].

The HP model has been found to have similar mutational properties compared to real proteins [42, 43]. A recent study on 2D HP-proteins with chain lengths ≤ 30 shows a single-mutation-induced fold switching [44], which has also been discovered in experimental studies [4, 45–50]. The main focus of this present article is on the study the effect of single-site substitution mutations on multiple HP sequences as a way of systematically approaching some of the questions introduced before on a very fundamental level. Therefore, we also introduce a new technique for independently estimating the complete density of states, including the ground-state degeneracy, during a generalized-ensemble simulation for which the simulation weights are determined using Wang–Landau sampling. A key to the efficiency of the approach is the encoding of a three dimensional HP-protein configuration uniquely into a serial direction sequence. This enables us to store and access the information of all visited structures efficiently during the simulation. In particular, the analysis of ground-state structures becomes feasible and can be carried out conveniently. In Sec. II, we will describe the model and method, results are presented in Sec. III and we conclude in Sec. IV.

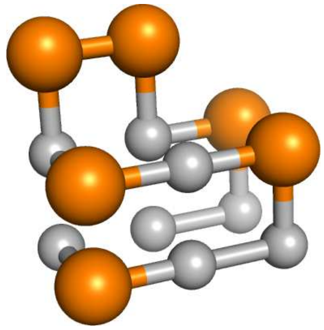

FIG. 1. (Color online) A 3D structure of a HP protein with 8 hydrophobic (H, silver) and 6 polar (P, orange) residues.

II. MODEL AND METHODS

A. The HP Lattice Model

The HP lattice model is a coarse-grained protein model which classifies amino acids into just two types, hydrophobic (H) and polar (P). Each amino acid in this model is represented as a single monomer on a simple cubic lattice. The hydrophobic interaction, as the key driving force of protein folding and tertiary structure formation [51, 52], is characterized by an effective monomer–monomer coupling ϵ_{HH} between non-bonded nearest-neighbor H monomers. The Hamiltonian is given by

$$\mathcal{H} = -\epsilon_{\mathrm{HH}} n_{\mathrm{HH}}\,, \tag{1}$$

where n_{HH} is the number of non-bonded HH contacts. Hence, the ground state, i.e., lowest-energy state, of a HP protein is the state with a maximum number of n_{HH}. See Fig. 1 for a sample visualization of a small HP ground state structure with $n_{\mathrm{HH}} = 8$.

B. Wang–Landau Sampling and Trial Moves

Wang–Landau sampling [39] is a Monte Carlo (MC) method which aims to estimate the density of states $g(E)$ while ideally performing a random walk in energy space. The acceptance probability for a MC trial move that changes the energy of the system from E_A to E_B is given by

$$P(A \to B) = \min\left\{1, \frac{g'(E_A)}{g'(E_B)}\right\}\,. \tag{2}$$

Upon acceptance, the estimator $g'(E)$ for the density of states is updated via $g'(E_B) \to f \times g'(E_B)$, where f is a modification factor, and the histogram of visited energies is increased by $H(E_B) \to H(E_B) + 1$. If the trial move was rejected, $g'(E_A)$ and $H(E_A)$ are updated instead in the same way. Once $H(E)$ is 'flat', the modification factor f will be reduced and all histogram entries will be reset to zero. The method performs this procedure iteratively until f is less than some pre-defined threshold value f_{final}. Even though multiple improvements of the details of this sampling method exist, we stick to the original procedure, where the initial modifications factor is set to $f_{\mathrm{init}} = \mathrm{e}^1$ and decreased via $\ln f \to \ln f/2$, and $\ln f_{\mathrm{final}} = 10^{-8}$. The initial guess for $g'(E)$ is $g'(E) = 1$ and we use the '80%' flatness criterion for the histogram $H(E)$. That is, all $H(E)$ entries are no less than 80% of the mean histogram height. Eventually, if we avoid potential systematic errors, $g'(E)$ will converge to the true $g(E)$ [53].

The trial moves we adopted in our simulation are pull moves [54] and bond-rebridging moves [55]. It has been found that these two trial moves work amazingly well with Wang–Landau sampling for both the determination of the minimum energy state and the estimation of density of states for the model used here [40, 41]. In our simulation, we used move fractions of 75% and 25% for pull moves and bond-rebridging moves, respectively.

C. Thermodynamic and Structural Quantities

The partition function $Z(T)$ of the system at a particular temperature T can be obtained with the knowledge of the density of states $g(E)$:

$$Z(T) = \sum_E g(E)\,\mathrm{e}^{-E/k_{\mathrm{B}}T}\,, \tag{3}$$

where k_{B} is the Boltzmann constant. This allows us to calculate the thermal properties such as the mean energy $\langle E\rangle(T)$, the heat capacity $C_V(T)$ and the ground-state population $P_0(T)$ [44]:

$$C_V(T) = \frac{\langle E^2\rangle - \langle E\rangle^2}{k_{\mathrm{B}}T^2} \tag{4}$$

$$P_0(T) = \frac{g(E_0)\,\mathrm{e}^{-E_0/k_{\mathrm{B}}T}}{Z(T)}, \tag{5}$$

where E_0 is the ground-state energy. As is common when studying generic models, we will work in reduced units in the following, i.e., we set $k_{\mathrm{B}} = 1$ and $\epsilon_{\mathrm{HH}} = 1$.

Besides those thermodynamic quantities, structural observables are also important in understanding the conformational changes during the folding process. We measure two commonly used quantities, radius of gyration (R_{g}) and end-to-end distance (R_{ee}):

$$R_{\mathrm{g}} = \left(\frac{1}{N}\sum_{i=1}^{N}(\vec{r}_i - \vec{r}_{\mathrm{cm}})^2\right)^{1/2} \tag{6}$$

$$R_{\mathrm{ee}} = |\vec{r}_N - \vec{r}_1|\,, \tag{7}$$

N is the number of monomers in the chain; $\vec{r}_i$ and $\vec{r}_{\mathrm{cm}}$ represent the positions of the ith monomer and the center of mass of the given configuration, respectively.

In addition, Wüst et al. [41] proposed another scalar structural observable, the tortuosity τ of the protein:

$$\tau = \left(\frac{1}{N-2} \sum_{i=1}^{N-2} (s_i - \overline{s})^2 \right)^{1/2} \tag{8}$$

where

$$s_i = \sum_{j=1}^{i} \vec{r}_{j,j+1} \times \vec{r}_{j,j+2} \,, \quad 1 \leq i \leq N-2 \,. \tag{9}$$

$\vec{r}_{j,j+1}$ denotes a two-dimensional vector in the plane defined by monomers j, $j+1$, and $j+2$. Unlike the radius of gyration and the end-to-end distance, which measure spatial extent only, τ is particularly sensitive to sequence-dependent internal topological features such as the breaking of HH contacts in compact denatured states upon folding to the ground state. For our purpose, it serves as a complementary structural quantity to better interpret features in the specific heat curves, for example. See also [41] for a discussion of this observable in the context of lattice polymers. To generally obtain more accurate structural quantities, we adopt the Wang–Landau resampling procedure, also proposed in [41].

D. Characterization of Ground-state Structures

One of the difficulties included in studying the ground state properties of proteins in the HP model (especially for long sequences) is the enormous degeneracy and high symmetry on the simple cubic lattice. Here we devise a simple heuristic method to characterize and store ground state structures during the simulation.

1. Sequence of Directions

For a given HP protein conformation on the simple cubic lattice, the "path" from the first monomer through the end can be uniquely recorded as a sequence of directions. We define two sets of values, $\vec{B}_1, \vec{B}_2, \ldots, \vec{B}_{N-1}$ and $D_1, D_2, \ldots, D_{N-1}$, for the $N-1$ bonds that connect consecutive monomers in a sequence of length N. The former one, for instance $\vec{B}_k$, is determined by the difference of coordinates between monomer k and $k+1$. Therefore $\vec{B}_k$ will be assigned one of values from $\{+\vec{X}, -\vec{X}, +\vec{Y}, -\vec{Y}, +\vec{Z}, -\vec{Z}\}$, where $+\vec{X}$ denotes positive X-axis direction, etc. The latter one is the sequence of direction (SoD), which contains five elements: *Forward*(F), *Left*(L), *Right*(R), *Up*(U) and *Down*(D) (see [56, 57] for similar representations). The procedure of calculating the sequence of directions can be described as follows:

1. Along the HP chain, pick the first three bonds $(1, i, j)$ which are all perpendicular to each other, i.e., such that $\vec{B}_1 \perp \vec{B}_i \perp \vec{B}_j \perp \vec{B}_1$.
2. Then $\vec{B}_1$, $\vec{B}_i$ and $\vec{B}_j$ define a new coordinate system (i.e., new directions $+\vec{X}$, $+\vec{Y}$, and $+\vec{Z}$) in which we calculate the remaining bonds.
3. The first bond (D_1) is, by definition, the *Forward* direction, while the next non-forward bond (D_i) is defined as *Left*. The other directions are then determined in step 4.
4. Assign F to $D_2 \ldots D_{i-1}$ and calculate D_h, $i < h < N$:

$$D_h = \begin{cases} F, & \text{IF} \quad \vec{B}_h = \vec{B}_{h-1} \\ L, & \text{ELIF} \quad \vec{B}_h = \vec{B}_{h-k} \\ & \text{AND} \quad o(\vec{B}_{h-1}, \vec{B}_h) = s(\vec{B}_{h-1}, \vec{B}_h) \\ R, & \text{ELIF} \quad \vec{B}_h = \vec{B}_{h-k} \\ & \text{AND} \quad o(\vec{B}_{h-1}, \vec{B}_h) \neq s(\vec{B}_{h-1}, \vec{B}_h) \\ U, & \text{ELIF} \quad o(\vec{B}_{h-k}, \vec{B}_{h-1}) = s(\vec{B}_{h-1}, \vec{B}_h) \\ & \text{AND} \quad s(\vec{B}_h, +) = 1 \\ U, & \text{ELIF} \quad o(\vec{B}_{h-k}, \vec{B}_{h-1}) \neq s(\vec{B}_{h-1}, \vec{B}_h) \\ & \text{AND} \quad s(\vec{B}_h, -) = 1 \\ D, & \text{ELIF} \quad o(\vec{B}_{h-k}, \vec{B}_{h-1}) = s(\vec{B}_{h-1}, \vec{B}_h) \\ & \text{AND} \quad s(\vec{B}_h, -) = 1 \\ D, & \text{ELIF} \quad o(\vec{B}_{h-k}, \vec{B}_{h-1}) \neq s(\vec{B}_{h-1}, \vec{B}_h) \\ & \text{AND} \quad s(\vec{B}_h, +) = 1 \end{cases}$$

where $\vec{B}_{h-k}$ is the closest preceding element that satisfy $\vec{B}_{h-k} \neq \vec{B}_{h-1}$ and $o(\vec{B}_m, \vec{B}_n)$, $s(\vec{B}_m, \vec{B}_n)$ are functions defined below:

$$o(\vec{B}_m, \vec{B}_n) = \begin{cases} 1\,, & \left(\left|\vec{B}_m\right|, \left|\vec{B}_n\right|\right) \in \{(X,Y),(Y,Z),(Z,X)\} \\ 0\,, & \text{otherwise} \end{cases}$$

$$s(\vec{B}_m, \vec{B}_n) = \begin{cases} 1\,, & \vec{B}_m, \vec{B}_n \text{ have the same sign} \\ 0\,, & \text{otherwise} \end{cases}$$

By this procedure we uniquely assign a SoD to each conformation and vice versa, taking the symmetries into account. That is, conformations are equal (modulo symmetry transformation of the cubic lattice) *iff* their SoD are identical.

2. Ground-State Sampling

To obtain all the ground state structures of a given HP sequence we perform a multicanonical sampling [58] on the whole energy space. During that process, trial states are generated as before and also accepted or rejected according to Eq. (2), where $g(E)$ is now the final estimator obtained from the preceding Wang–Landau run and not updated anymore. If the putative ground-state energy, i.e., the lowest energy found during the Wang–Landau run, is met, we calculate the direction sequence of this state and compare it to those of previously found ground-state structures, which we store in a tree structure container with a branching factor of at most five (the number of elements in an SoD). In this tree data structure, a direction sequence is uniquely represented by a path of length $N-1$ from the root node to a leaf node. Hence, the complexity of verifying a new found direction sequence is $\mathcal{O}(N)$ [59]. If the actual ground state is already present in that container, we just proceed. Otherwise, the new structure will be added to the database and the counter of degeneracy increased. The simulation ideally ends when the rate of finding new ground states approaches zero, i.e, the estimator for the ground-state degeneracy converges. In practice, we terminate the runs after a predefined number of MC steps (see below). Note that even though we will use this method mainly to estimate ground-state degeneracies, it is of course applicable to any other energy level just as well.

III. RESULTS AND DISCUSSION

A. Ground State Structure Searching

As a verification of our method, we chose 4 prominent HP sequences with length of 14, all of which have been studied using an enumeration method [21], and performed a multicanonical scan counting the absolute density of states. That is, we estimate the degeneracy of all energy levels analogously to the ground-state sampling described above. The results are shown in Table I, where the numbers of unique structures at each energy level are given. By identifying the dimension of each structure and considering different symmetries ($1\mathrm{D}\times 6; 2\mathrm{D}\times 24; 3\mathrm{D}\times 48$), we calculated the densities of states and found them to be exactly the same compared to enumeration results [21]. Each of these simulations took less than 4×10^9 Monte Carlo steps for $g(E_0)$ to converge.

After this proof of concept, some other widely studied HP sequences [56, 60, 61] have been chosen for testing our scheme. We carried out simulations for estimating the ground-state degeneracy for each of these sequences, and listed the results in Table II. For short sequences (e.g. 27.2, 27.3 and 31) or sequences with low ground-state degeneracy (e.g. 42 and 67), the results of our simulation agree with other studies perfectly. Due to the high ground-state degeneracy, it is extremely challenging to reach all ground states for the 48mers [61] in finite simulation time (we ran up to 2.5×10^{11} MC steps). However, there are two sequences (48.3 and 48.9) for which the ground-state degeneracy stayed stable for a long time, and we thus believe we have converged to the true value $g(E_0)$. By normalizing the number of ground states and Monte Carlo time, we find that these two sequences share the same convergence behavior. The assumption of a fundamental convergence pattern provides a means to extrapolate the true ground-state degeneracy for other long sequences. Hence, we fitted the normalized number of visited, different ground-states vs. time

TABLE I. Our Monte Carlo results for absolute densities of states for four 14mers. Columns from left to right: energy level, total number of structures of all dimensions, 2D structures (n_{2D}), 3D structures (n_{3D}) and $g(E)=6\,n_{1D}+24\,n_{2D}+48\,n_{3D}$. Each sequence has only 1 1D-structure (with $E=0$) which is not shown. Our results are identical to results from exact enumeration [21].

SeqID: 14.1 (*HPHPHHPHPHHPPH*)				
E	All	n_{2D}	n_{3D}	$g(E)$
−8	1	0	1	48
−7	262	0	262	12 576
−6	3 380	5	3 375	162 120
−5	28 163	84	28 079	1 349 808
−4	176 076	713	175 363	8 434 536
−3	754 422	3 809	7 50 613	36 120 840
−2	2 466 457	14 059	2 452 398	118 052 520
−1	6 533 719	38 605	6 495 114	312 691 992
0	9 758 750	52 912	9 705 837	467 150 070
SUM	19 721 230			943 974 510

SeqID: 14.2 (*HHPPHPHPHHPHPH*)				
E	All	n_{2D}	n_{3D}	$g(E)$
−8	2	0	2	96
−7	220	0	220	10 560
−6	2 929	4	2 925	140 496
−5	22 738	68	22 670	1 089 792
−4	139 052	561	138 491	6 661 032
−3	625 336	3 014	622 322	29 943 792
−2	2 102 592	10 872	2 091 720	100 663 488
−1	5 710 617	31 935	5 678 682	273 343 176
0	11 117 744	63 733	11 054 010	532 122 078
SUM	19 721 230			943 974 510

SeqID: 14.3 (*HHPHPHPPHPHPHH*)				
E	All	n_{2D}	n_{3D}	$g(E)$
−8	2	0	2	96
−7	200	1	199	9 576
−6	2 631	2	2 629	126 240
−5	21 987	68	21 919	1 053 744
−4	125 858	510	125 348	6 028 944
−3	591 753	3 110	588 643	28 329 504
−2	2 286 507	13 296	2 273 211	109 433 232
−1	6 392 045	37 796	6 354 249	305 911 056
0	10 300 247	55 404	10 244 842	493 082 118
SUM	19 721 230			943 974 510

SeqID: 14.4 (*HHPHPPHPHPHHPH*)				
E	All	n_{2D}	n_{3D}	$g(E)$
−8	4	0	4	192
−7	232	0	232	11 136
−6	3 348	7	3 341	160 536
−5	26 267	74	26 193	1 259 040
−4	163 540	757	162 783	7 831 752
−3	801 505	4 370	797 135	38 367 360
−2	2 702 687	15 734	2 686 953	129 351 360
−1	6 575 905	39 087	6 536 818	314 705 352
0	9 447 742	50 158	9 397 583	452 287 782
SUM	19 721 230			943 974 510

TABLE II. Estimated ground-state degeneracy of some widely studied HP proteins. For each of them we listed the ground-state energy E_0, the ground-state degeneracy $g^{\mathrm{L}}(E_0)$ found in earlier studies and $g(E_0)$ estimated with our method. Converged sequences do not have statistical errors; otherwise error bars were obtained from multiple extrapolation fits (see text).

	SeqID	E_0	$g^{\mathrm{L}}(E_0)$	$g(E_0)$
1	27.1	-16	36691	51537
	27.2	-15	297	297
	27.3	-16	25554	25554
	31	-28	1114	1114
2	42	-34	4	4
	67	-56	3	3
3	48.1	-32	$(5.2 \pm 0.8) \times 10^6$	$(10.3 \pm 0.4) \times 10^6$
	48.2	-34	$(1.7 \pm 0.8) \times 10^4$	$(2.84 \pm 0.02) \times 10^4$
	48.3	-34	$(6.6 \pm 2.8) \times 10^3$	5.09×10^3
	48.4	-33	$(6.0 \pm 1.3) \times 10^4$	$(4.97 \pm 0.16) \times 10^4$
	48.5	-32	$(1.2 \pm 0.3) \times 10^6$	$(1.94 \pm 0.04) \times 10^6$
	48.6	-32	$(9.6 \pm 1.9) \times 10^4$	$(1.84 \pm 0.02) \times 10^6$
	48.7	-32	$(5.8 \pm 2.1) \times 10^4$	$(10.8 \pm 0.1) \times 10^4$
	48.8	-31	$(2.2 \pm 0.7) \times 10^7$	$(1.59 \pm 0.03) \times 10^7$
	48.9	-34	$(1.4 \pm 0.5) \times 10^3$	2.614×10^3
	48.10	-33	$(1.9 \pm 0.9) \times 10^5$	$(5.53 \pm 0.14) \times 10^5$

[1] values of $g^{\mathrm{L}}(E_0)$ can be referred to Yue and Dill [56].
[2] values of $g^{\mathrm{L}}(E_0)$ can be referred to Yue and Dill [60].
[3] values of $g^{\mathrm{L}}(E_0)$ can be referred to Bachmann and Janke [61]

for other sequences to the known curve for 48.3 and extrapolated their ground-state degeneracy. As an example, we show in Fig. 2 the corresponding fit for sequence 48.1. The extrapolated part is marked by the dashed line in the figure. However, instead of a unique fit, there are multiple choices which fit equally well. Therefore, by doing 20 different fits, the average value as well as an error bar could be calculated. Even though not every curve fits as well as Fig. 2, it provides a better estimation of the true value $g(E_0)$. We note that our procedure yields rather different values than those obtained earlier using an approach where $g(E_0)$ is obtained from an implicit estimate of the partition function [61]. However, since our estimates are obtained from explicit enumeration of ground states with very high statistics, we believe that our procedure provides more reliable results.

B. Effect of Single-Site Mutations

After this instructive preparatory work, we now focus on the main part of this study: the effect of single-site mutations on ground states and the thermodynamic behavior of HP proteins. A single-site mutation (SSM) on a HP protein consists of a 'flip' of one monomer from its original type to the other. For example, HP**H**HP becomes HP**P**HP under SSM on the third monomer. To understand possible effects of SSM on HP proteins, we choose two sequences which were designed to study the origins of tertiary structures in proteins [60]:

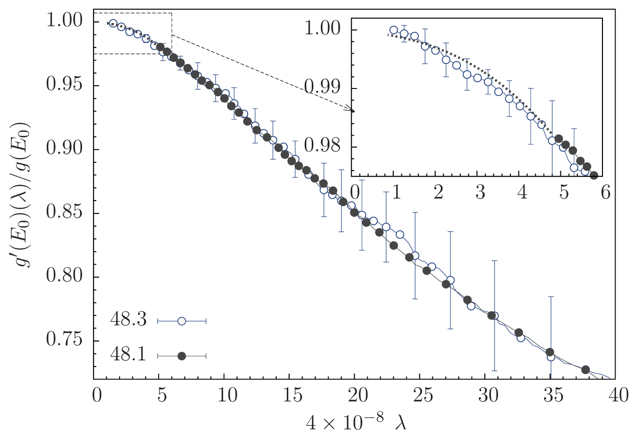

FIG. 2. (Color online) Number of different ground-states found over time for HP sequences 48.1 fitted to the corresponding curve of protein 48.3. $g'(E_0)(\lambda)$ is the actual estimator of GS degeneracy and $\lambda = 1/(10000$ MC Steps$)$ is the inverse Monte Carlo time. For clarity, only selected data points and error bars are shown. See text for details.

$$
\begin{aligned}
\text{Seq3D42}: &\quad \mathrm{P(H(HP)_2)_2HP_2H_3(PH)_2\ (HP)_2H_3P_2H((PH)_2H)_2P} \\
\text{Seq3D67}: &\quad \mathrm{(PH(PH_2)_2PHP_2H_3PP)_3PH(PH_2)_2PHP_2H_3P} \\
&\quad \equiv \mathrm{xPxPxPx}, \text{ where } \mathrm{x=PH(PH_2)_2PHP_2H_3P}
\end{aligned}
$$

There are symmetries present in these two sequences: Seq3D42 reads the same forward and backwards, and Seq3D67 is composed of four identical pieces, each pair of which is connected through a P monomer. The ground state structures of these two lattice proteins mimic by construction α/β-barrels and the β-helix, respectively (see App. A). Note that the ground-state degeneracy is extremely small (Table II). The SSM have been systematically performed on each monomer of both HP chains. We thus create 42 and 67 mutated sequences, respectively. We denote Seq3D42sk as the mutated sequence generated by applying SSM on kth monomer of Seq3D42 (and analogously for Seq3D67). We performed simulations of each of these mutated sequences independently as described earlier. Results are shown and discussed in the following.

1. Ground States

We are first interested in how the SSM affect the ground states (GS) of HP proteins in terms of their energy, actual conformations and degeneracy. In Figs. 3 and 4 we plot the ground-state energy and degeneracy for all SSM mutations of Seq3D42 and Seq3D67, respectively. For both sequences we find that the effect of SSM can vary significantly, depending on the monomer position. About half of the mutated sequences retain their

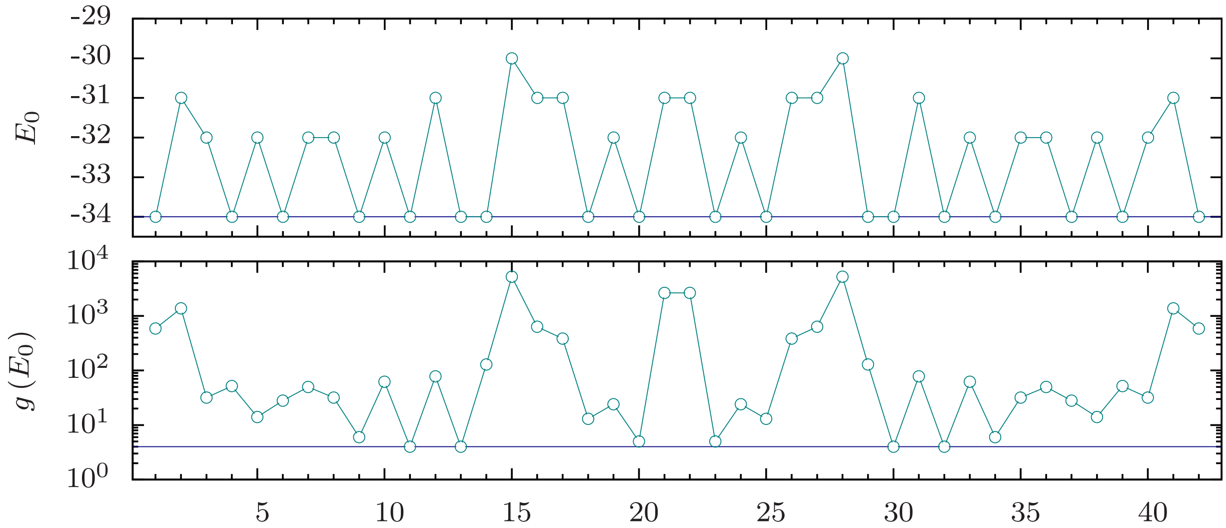

FIG. 3. (Color online) Ground-state energy E_0 (top panel) and ground-state degeneracy $g(E_0)$ (bottom panel) of mutated Seq3D42. The X-axis value indicates the position which has been affected by the single-site mutation. Properties of the original, unmutated sequence are marked by horizontal lines.

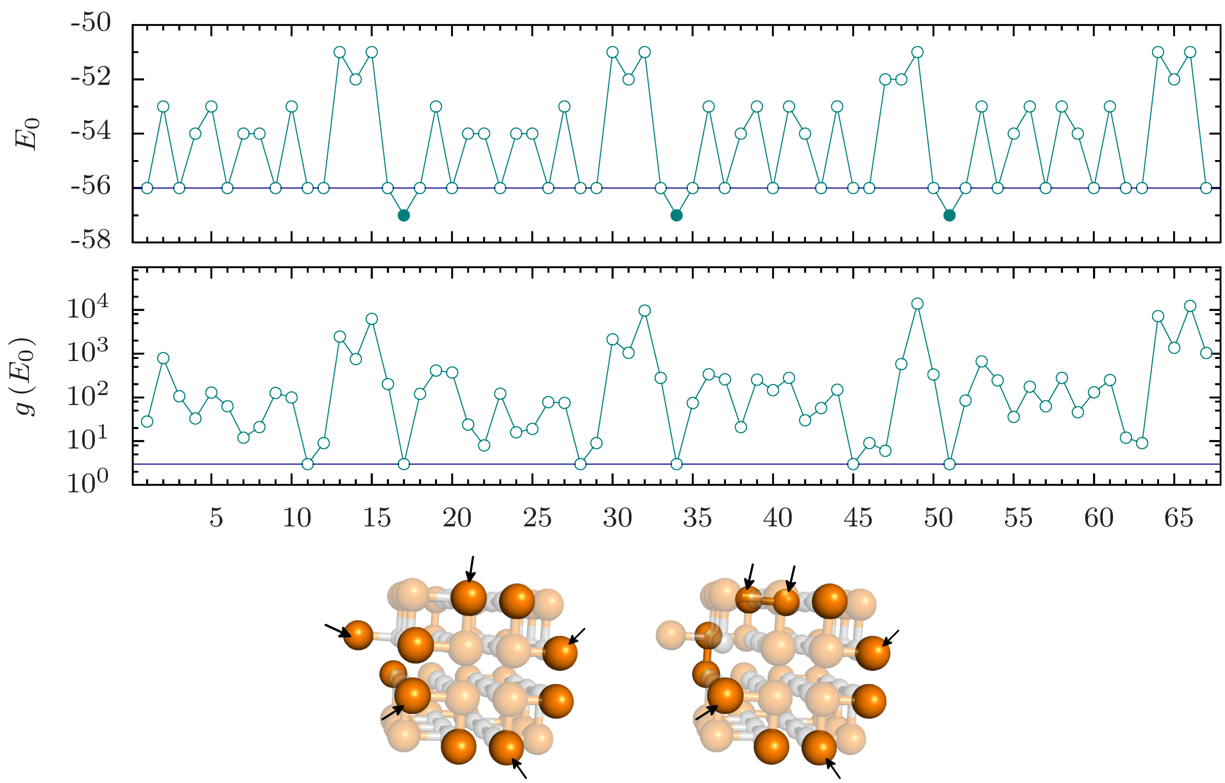

FIG. 4. (Color online) Ground-state energy E_0 and ground-state degeneracy $g(E_0)$ of mutated Seq3D67 (cp. Fig. 3). (Color online) Each of the bottom pictures shows the result of two overlapping ground-state structures of Seq3D67. Overlapped monomers are shown in dim color. Monomers pointed to by arrows belong to the same structure, while the rest belong to different structures.

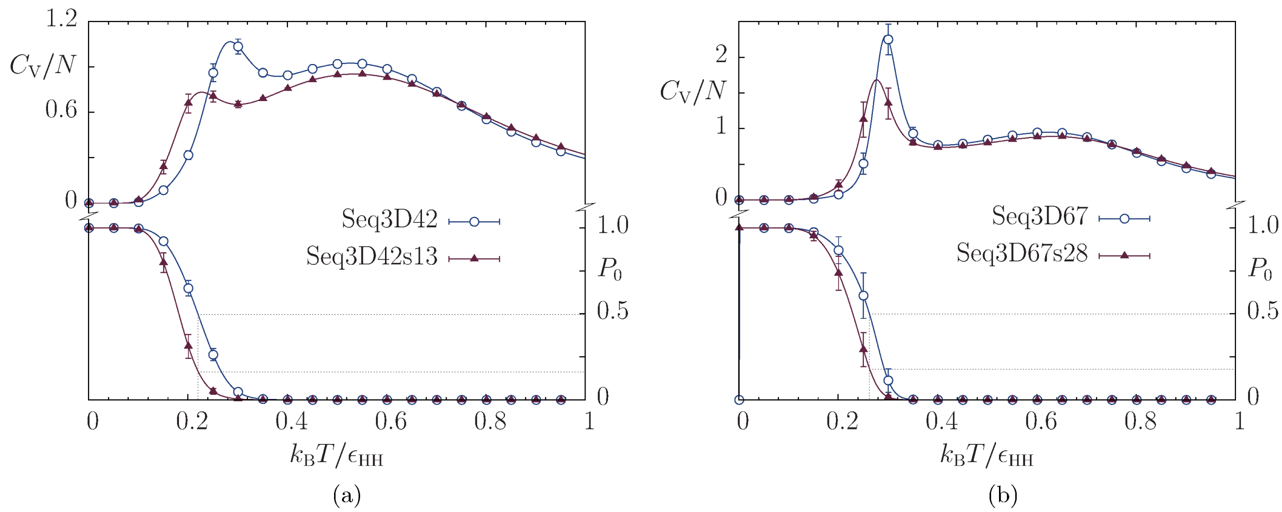

FIG. 5. (Color online) Examples: Thermal stability of ground state (a) Comparison between Seq3D42s13 and Seq3D42 based on specific heat (top curves, left scales) and ground-state population (bottom curves, right scales) . (b) Comparison between Seq3D67s28 and Seq3D67 based on specific heat and ground-state population . In both figures, error bars smaller than data points are not shown.

ground-state energy (GSE), while others changed significantly. For example, mutations on the 15th monomer of Seq3D42 or the 13th of Seq3D67 change the GSE from $E = -34$ to -30 and from $E = -56$ to -51, respectively. Moreover, three mutated sequences (Seq3D67s17, Seq3D67s34 and Seq3D67s51) even have lower GSE ($E = -57$) compared to the original sequence. Interestingly, none of the mutated sequences has a GSE of $E = -33$ or -55, which correspond to the first excited states of the unmutated Seq3D42 and Seq3D67, respectively.

Regarding the ground-state degeneracy (GSD), most of the mutated sequences show dramatically larger values than the unmutated ones. However, by comparing their ground-state structures, we found that 88 out of 109 (36 for the 42mer and 52 for the 67mer) mutated sequences retain the ground-state structures of the original sequence. For Seq3D67 we identified six P monomers (at positions 11, 17, 28, 34, 45 and 51; cp. Fig. 4) which are “immune” against SSM in the sense that the ground-state degeneracy and the actual ground-state structures stay exactly the same except for the substituted site. For three of them (17, 34, and 51) SSM even results in lower ground-state energy. Furthermore, we saw that the ground states remain unaffected under multiple site mutations, i.e., mutating up to all three sites simultaneously. We also find sequences where a single-site mutation does not affect the ground-state energy but its degeneracy. In these cases we observe that SSM lowers the thermal stability of ground states by notably increasing the degeneracy of the first excited states, for example. Through examining the 3D ground state structures of the 67mer, we found that these “immune” positions are at the joints of lattice helices and lattice strands, while those extremely sensitive sites (e.g. 15, 32, 49) are usually located at the lattice strands (cp. App. A). We note that the symmetries observed in Fig. 3 reflect the symmetry in the HP sequence of Seq3D42 as expected, providing further evidence for the validity of our method.

In Fig. 5, we plot the specific heat $C_V(T)/N$ and the ground-state population $P_0(T)$ (Eqs. (4) and (5)) of two sequences for which both the ground-state energy and degeneracy does not change compared to the corresponding unmutated sequence. We see a shift of the ground-state population P_0 to lower temperatures. For example, at the temperature where 50% of the conformations in the canonical distributions of the unmutated sequences correspond to ground-states, this percentage drops to 17%–18% for both mutated sequences (see grid-lines in Fig. 5). That is, the ground-state population is much more sensitive to temperature increase compared to the original protein. Looking at the heat capacity, we also note a shift of the low-energy peak which corresponds to the formation of the compact hydrophobic core, i.e., this core breaks apart at lower temperatures as an effect of the mutation. Both observations show that the mutations lower the thermal stability of the ground-states of the investigated HP proteins.

2. *Thermodynamic and structural properties*

Finally, we investigate in more detail how single-site mutations can affect the thermal behavior of HP proteins. Such knowledge could help unveiling the effect of mutations on the folding process, for example. The quantities we are interested in here are the specific heat, the end-to-end distance, the tortuosity and the radius of gyration, as defined Sec. II C.

By examining all mutated sequences of Seq3D42 and (most of) Seq3D67, we have discovered cases where all

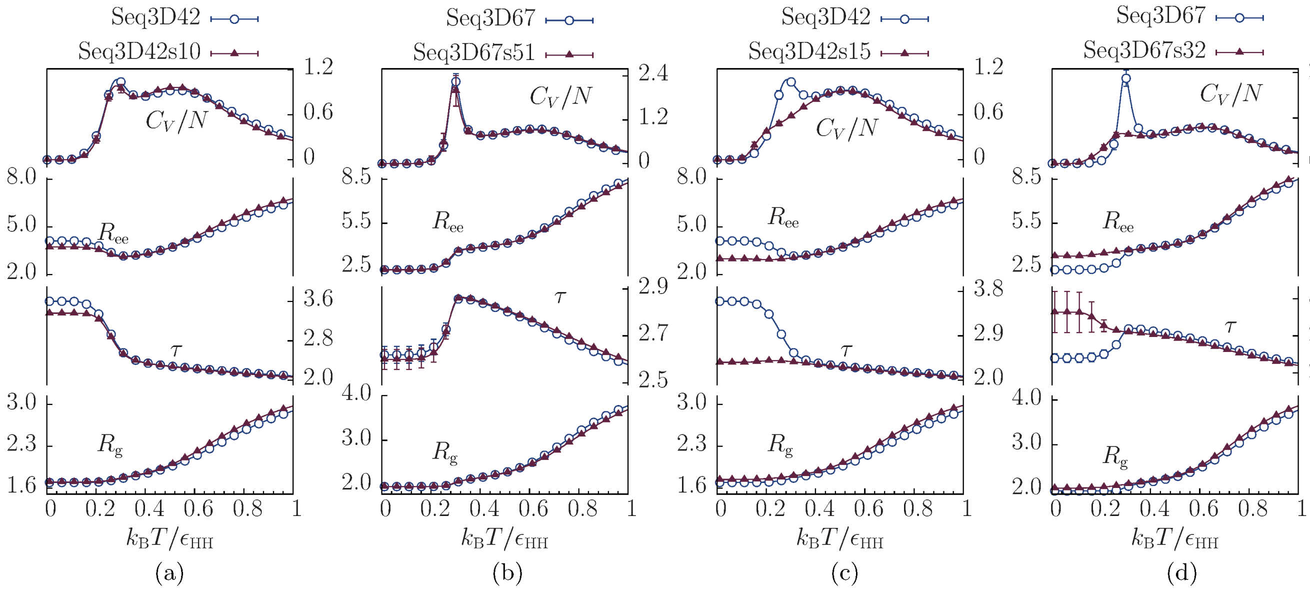

FIG. 6. (Color online) Effect of mutation on folding behavior. (a) and (b) are two cases where the mutations do not affect the folding behavior while (c) and (d) are examples of changed thermodynamic quantities under mutation. In all figures above, error bars smaller than data points are not shown.

quantities revealed very similar behavior compared to the unmutated sequences (see Figs. 6 a and b). This comparison strongly indicates that those mutations do not affect the folding behavior significantly. More than 50% of all single-site mutations fall into this class, in which sequences contain the original ground-state structures and add, if at all, only a small number to the ground-state degeneracy. On the other hand, there are instances where mutations significantly affect thermal quantities. As shown in Fig. 6 (c) and (d), mutated sequences can present different behaviors in various ways. Typically, the left peak of heat capacity, which corresponds to the hydrophobic core formation (see, for example, Ref. [61] for a more detailed discussion of this transition), becomes lower or fades into a shoulder, along with raised or lowered τ and $R_{\rm ee}$. Significant change of $R_{\rm g}$ has not been observed in all of our cases, which implies that this quantity is, not surprisingly for this model, quite stable under single-site mutation. Under this type of effects, mutated sequences also show up with sharp increase in ground-state degeneracy and might lose the original ground-state structures.

IV. SUMMARY AND CONCLUSION

The effect of mutations on proteins is of fundamental interest in many areas of life sciences. There are different approaches to study this effect by means of computer simulations, leading to complementary insights: one could choose an atomistic model for a specific protein and study a specific mutation, or one could choose generic models and perform systematic studies of general mechanisms. There have been a number of works for the latter approach [22, 42–44], but for the first time, we provide a conclusive and reliable method to systematically and thoroughly study mutations on large lattice-proteins, i.e., proteins that are larger than ~ 30 monomers, which will not be accessible for exact enumeration anytime soon.

Our heuristic method estimates the density of states, including the absolute ground-state degeneracy, of HP lattice proteins. It combines flat-histogram sampling with an efficient structure database and enables us to gain detailed insight in systems of sizes far beyond those accessible by enumeration approaches, while also working as effectively as such methods for short HP sequences. Moreover, Wang–Landau sampling with appropriate trial moves has proven to be successful in ground state searching for HP sequences as long as 136 [41]. Therefore we believe our method should be at least suitable for sequences with this length. To demonstrate the usefulness of this new method, we apply it for a thorough investigation of the effect of single-site mutation on two long, designed HP proteins and discovered that many mutations do not affect the protein significantly in any regard, including the ground-state degeneracy and energy. On the other hand, very sensitive positions in the primary structure exist, where mutations can drastically change the folding process and low-energy structures. Remarkably, both observations coincide with experimental discoveries for real proteins [5, 7], as discussed in Sec. I, confirming the adequacy of simple, generic models for certain problems. In addition, we found that the thermal stability of mutated sequences is likely to be lower than original sequences, from the observation of ground-state population and specific heat. The reason is that even though the ground-state degeneracy may increase dramatically after mutations, the degeneracy of the first and second excited states grow with the same rate or even faster.

ACKNOWLEDGMENTS

We thank M. Bachmann for constructive discussions. This work was supported by the National Science Foundation under Grant No. DMR-0810223 and No. OCI-0904685. LA-UR-14-21619 assigned. Y.W. Li was sponsored by the Office of Advanced Scientific Computing Research; U.S. Department of Energy. Part of the work was carried out at the Oak Ridge National Laboratory, which is managed by UT-Battelle, LLC under Contract No. De-AC05-00OR22725. Computing resources were partially provided by the Georgia Advanced Computing Resource Center and the Texas Advanced Computing Center under XSEDE Grant No. PHY130014.

[1] K. A. Dill and J. L. MacCallum, Science **338**, 1042 (2012).
[2] A. R. Davidson, Proc. Natl. Acad. Sci. **105**, 2759 (2008).
[3] C. G. Roessler, B. M. Hall, W. J. Anderson, W. M. Ingram, S. A. Roberts, W. R. Montfort, and M. H. J. Cordes, Proc. Natl. Acad. Sci. **105**, 2343 (2008).
[4] P. A. Alexander, Y. He, Y. Chen, J. Orban, and P. N. Bryan, Proc. Natl. Acad. Sci. **104**, 11963 (2007).
[5] S. Rackovsky, Phys. Rev. Lett. **106**, 248101 (2011).
[6] J. H. Miller, C. Coulondre, M. Hofer, U. Schmeissner, H. Sommer, A. Schmitz, and P. Lu, J. Mol. Biol. **131**, 191 (1979).
[7] J. U. Bowie, J. F. Reidhaar-Olson, W. A. Lim, and R. T. Sauer, Science **247**, 1306 (1990).
[8] K. A. Dill, Protein Sci. **8**, 1166 (1999).
[9] A. Kolinski and J. Skolnick, Polymer **45**, 511 (2004).
[10] K. A. Dill, Biochemistry **24**, 1501 (1985).
[11] K. F. Lau and K. A. Dill, Macromolecules **22**, 3986 (1989).
[12] V. Castells, S. Yang, and P. Van Tassel, Phys. Rev. E **65**, 031912 (2002).
[13] M. Bachmann and W. Janke, Phys. Rev. E **73**, 020901 (2006).
[14] A. Swetnam and M. P. Allen, Phys. Rev. E **85**, 062901 (2012).
[15] M. Radhakrishna, S. Sharma, and S. K. Kumar, J. Chem. Phys. **136**, 114114 (2012).
[16] Y. W. Li, T. Wüst, and D. P. Landau, Phys. Rev. E **87**, 012706 (2013).
[17] R. Bonaccini and F. Seno, Phys. Rev. E **60**, 7290 (1999).
[18] G. Ping, J. M. Yuan, M. Vallieres, H. Dong, Z. Sun, Y. Wei, F. Y. Li, and S. H. Lin, J. Chem. Phys. **118**, 8042 (2003).
[19] B. Pattanasiri, Y. W. Li, D. P. Landau, T. Wüst, and W. Triampo, J. Phys.: Conf. Ser. **402**, 012048 (2012).
[20] A. Irbäck and C. Troein, J. Biol. Phys. **28**, 1 (2002).
[21] M. Bachmann and W. Janke, Acta Phys. Pol. B **34**, 4689 (2003).
[22] R. Schiemann, M. Bachmann, and W. Janke, J. Chem. Phys. **122**, 114705 (2005).
[23] S. L. Narasimhan, A. K. Rajarajan, and L. Vardharaj, J. Chem. Phys. **137**, 115102 (2012).
[24] R. Backofen and S. Will, Constraints **11**, 5 (2006).
[25] E. M. O'Toole and A. Z. Panagiotopoulos, J. Chem. Phys. **97**, 8644 (1992).
[26] T. C. Beutler and K. A. Dill, Protein Sci. **5**, 2037 (1996).
[27] P. Grassberger, Phys. Rev. E **56**, 3682 (1997).
[28] H. Frauenkron, U. Bastolla, E. Gerstner, P. Grassberger, and W. Nadler, Phys. Rev. Lett. **80**, 3149 (1998).
[29] M. Bachmann and W. Janke, Phys. Rev. Lett. **91**, 208105 (2003).
[30] H.-P. Hsu, V. Mehra, W. Nadler, and P. Grassberger, J. Chem. Phys. **118**, 444 (2003); Phys. Rev. E **68**, 021113 (2003).
[31] T. Prellberg and J. Krawczyk, Phys. Rev. Lett. **92**, 120602 (2004).
[32] J. L. Zhang and J. S. Liu, J. Chem. Phys. **117**, 3492 (2002).
[33] J. Zhang, S. C. Kou, and J. S. Liu, J. Chem. Phys. **126**, 225101 (2007).
[34] W. Tang and Q. Zhou, Phys. Rev. E **86**, 031909 (2012).
[35] R. Unger and J. Moult, J. Mol. Biol. **231**, 75 (1993).
[36] R. König and T. Dandekar, BioSystems **50**, 17 (1999).
[37] F. Liang and W. H. Wong, J. Chem. Phys. **115**, 3374 (2001).
[38] A. Shmygelska and H. H. Hoos, BMC Bioinf. **6**, 30 (2005).
[39] F. Wang and D. P. Landau, Phys. Rev. Lett. **86**, 2050 (2001); Phys. Rev. E **64**, 1 (2001); D. P. Landau, S.-H. Tsai, and M. Exler, Am. J. Phys. **72**, 1294 (2004).
[40] T. Wüst and D. P. Landau, Phys. Rev. Lett. **102**, 178101 (2009).
[41] T. Wüst and D. P. Landau, J. Chem. Phys. **137**, 064903 (2012).
[42] K. F. Lau and K. A. Dill, Proc. Natl. Acad. Sci. **87**, 638 (1990).
[43] D. Shortle, H. S. Chan, and K. A. Dill, Protein Sci. **1**, 201 (1992).
[44] C. Holzgräfe, A. Irbäck, and C. Troein, J. Chem. Phys. **135**, 195101 (2011).
[45] F. J. Blanco, I. Angrand, and L. Serrano, J. Mol. Biol. **285**, 741 (1999).
[46] S. Dalal and L. Regan, Protein Sci. **9**, 1651 (2000).
[47] T. A. Anderson, M. H. J. Cordes, and R. T. Sauer, Proc. Natl. Acad. Sci. **102**, 18344 (2005).
[48] X. I. Ambroggio and B. Kuhlman, Curr. Opin. Struc. Biol. **16**, 525 (2006).
[49] Y. He, Y. Chen, P. Alexander, P. N. Bryan, and J. Orban, Proc. Natl. Acad. Sci. **105**, 14412 (2008).
[50] P. A. Alexander, Y. He, Y. Chen, J. Orban, and P. N. Bryan, Proc. Natl. Acad. Sci. **106**, 21149 (2009).
[51] W. Kauzmann, in *Advances in Protein Chemistry*, Vol. 14, edited by K. B. C.B. Anfinsen, M.L. Anson and J. T. Edsall (Academic Press, 1959) p. 1.
[52] K. A. Dill, Science **250**, 297 (1990).
[53] C. Zhou and R. N. Bhatt, Phys. Rev. E **72**, 025701 (2005).
[54] N. Lesh, M. Mitzenmacher, and S. Whitesides, in RECOMB (Berlin, Germany, 2003) , p. 188 (2003).
[55] J. M. Deutsch, J. Chem. Phys. **106**, 8849 (1997).
[56] K. Yue and K. A. Dill, Phys. Rev. E **48** (1993).
[57] R. Schiemann, M. Bachmann, and W. Janke, Comp. Phys. Comm. **166**, 8 (2005).
[58] B. A. Berg and T. Neuhaus, Phys. Rev. B **267**, 249 (1991); Phys. Rev. Lett. **68**, 9 (1992).
[59] T. H. Cormen, C. E. Leiserson, R. L. Rivest, and C. Stein, *Introduction to Algorithms, 3rd ed.* (MIT Press, Cambridge, MA, 2009).
[60] K. Yue and K. A. Dill, Proc. Natl. Acad. Sci. **92**, 146 (1995).
[61] M. Bachmann and W. Janke, J. Chem. Phys. **120**, 6779 (2004).

Appendix A: Ground State Structures

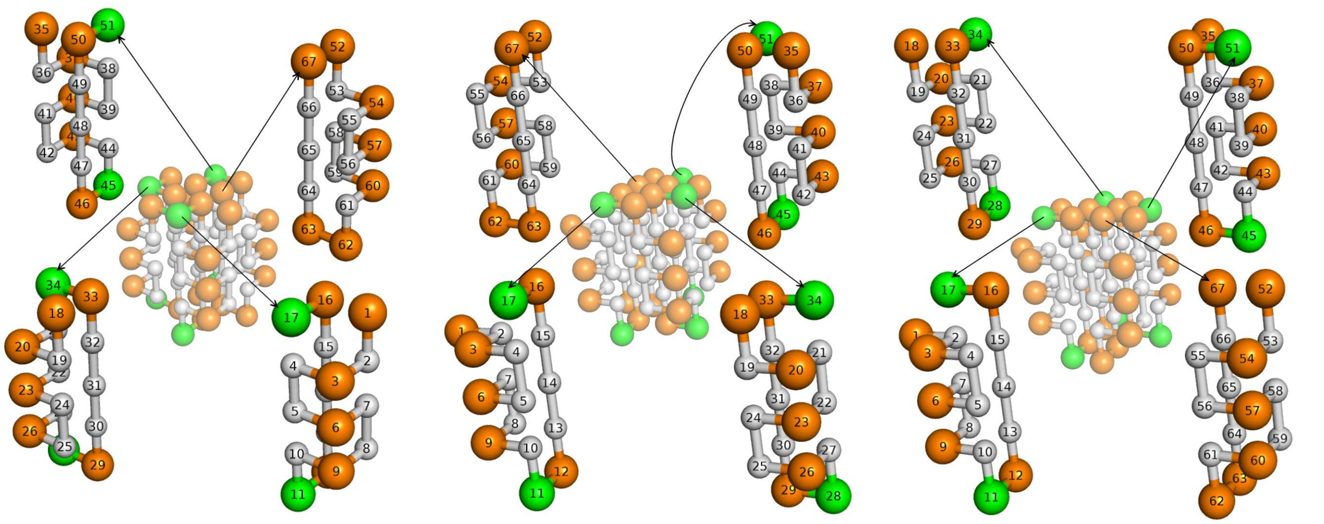

(a) (b) (c)

FIG. 7. (Color online) Three different ground state structures for the 67mer studied in this paper. Residues 2-10 form a lattice helix, and residues 12-16 form a lattice strand [60]. Hydrhophobic monomers are colored in silver, while polar monomers are either orange or green. Green colored monomers are those for which the ground state degeneracy remains the same under single-site mutation. And these monomers are also at the joints of lattice strands and lattice helices.

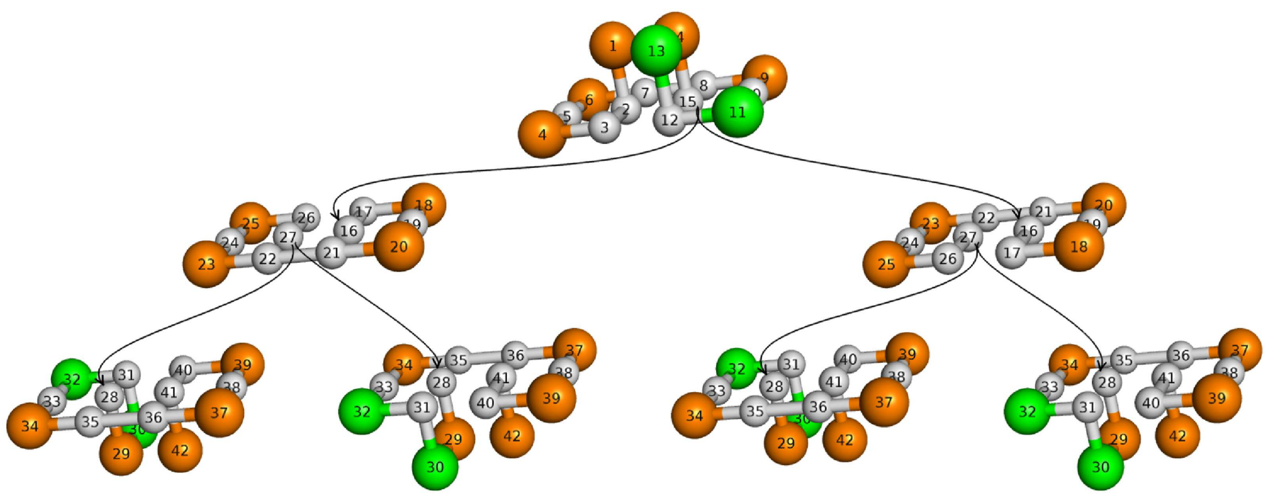

(a) (b) (c) (d)

FIG. 8. (Color online) Four different ground state structures for the 42mer studied in this paper. Each ground state structure is sliced into three layers. The top layer is shared by all the ground state structures, while there are two different structures for middle and for bottom layers respectively. Arrows in the figure pointed to the bonded monomer in the next layer. Hydrhophobic monomers are colored in silver, while polar monomers are either orange or green. Green colored monomers are those for which the ground state degeneracy remains the same under single-site mutation.